SEVERE ACCIDENT EVALUATIONS FOR CONVENTIONAL PWR POWER PLANT WITH SIC COMPOSITE FUEL CLADDING

Y. YAMAKOSHI, K. KIRIMURA, H. KURAMOTO, T. NODA
Mitsubishi Heavy Industries, Ltd.
1-1, Wadasaki-Cho 1-Chome, Hyogo-Ku, Kobe 652-8585, Japan

S. YAMASHITA, T. FUKAHORI
Japan Atomic Energy Agency
2-4, Ooaza Shirakata, Tokai-Mura, Naka-Gun, Ibaraki-Ken 319-1195, Japan

ABSTRACT

Silicon carbide (SiC) composite fuel cladding as accident tolerant fuel cladding has been studied for many years. Since SiC fuel cladding is characterized by a low oxidation reaction rate, it is expected that core heat up is delayed during severe accident (SA), leading to a longer time-of-grace before core melt and to low hydrogen generation. In this study, SA analyses are performed for conventional pressurized water reactors (PWR) with SiC composite fuel cladding in order to confirm the merit of SiC fuel cladding compared to current fuel cladding in terms of time to core melt and hydrogen generation.

In the SA analyses, small break loss of coolant accident (LOCA) sequences are selected because they are dominant sequences in the total core damage frequency of Japanese PWR. The accident progression of small break LOCA sequences are more moderate than large break LOCA sequences, so that the merit of SiC in the SA conditions can be shown more clearly. According to the SA analyses using MELCOR, the timing of the core melt for SiC fuel cladding is delayed by a few hours compared to current fuel cladding. In addition, the hydrogen generation for SiC fuel cladding is reduced compared to current fuel cladding. Hence the merit of SiC fuel cladding is shown especially for small break LOCA sequences.

This study is the result of “Development of Technical Basis for Introducing Advanced Fuels Contributing to Safety Improvement of Current Light Water Reactors” which is carried out under the Project on Development of Technical Basis for Improving Nuclear Safety by the Ministry of Economy, Trade and Industry of Japan.

Keywords**:** ATF, SiC, cladding, severe accident, PWR

1. Introduction

With this material as accident tolerant fuel (ATF) cladding, core melt could be delayed by several minutes or hours, during which emergency core cooling system (ECCS) can be recovered.

In the Japanese PWR plants, small break LOCAs as initiating events are dominant sequences of their total core damage frequency (CDF). It is therefore appropriate to evaluate the advantage of SiC for small break LOCAs. The advantages of SiC are shown by SA evaluations using MELCOR. MELCOR is modeled for current fuel cladding, so material properties and oxidation reaction rate are changed by input parameters in order to model SiC.

In this paper, the results of SA analyses for SiC fuel cladding are described and the advantages of SiC fuel cladding are discussed.

2. Method for Modeling SiC in the MELCOR

In this section, the method for modeling SiC in the MELCOR is described. MELCOR is developed for current fuel cladding. In order to model SiC, the inputs of the MELCOR are changed.

First, material properties are changed from current fuel cladding to SiC. Table 1 shows the material properties of SiC [1][2]. Material properties to be changed include the melting point, density, specific heat, thermal conductivity, and latent heat of fusion. There is no data for latent heat of fusion, so a provisional value is used for the latent heat of fusion.

Table 1 Material properties of SiC

Material properties	Value	Remarks
Melting point	2818.15 K	[1]
Density	2500 kg/m^3	Averaged data [2]
Specific heat	1300 J/kg/K	Value at high temperature [1]
Thermal conductivity	3 W /m/K	Value calculated from the data [2]
Latent heat of fusion	$1x10^6$ J/kg	Provisional value

Second, oxidation reaction rates are changed from current fuel cladding to SiC. Figure 1 shows the schematic diagram of SiC oxidation and SiO_2 volatilization. The symbols in this figure are as below [3].

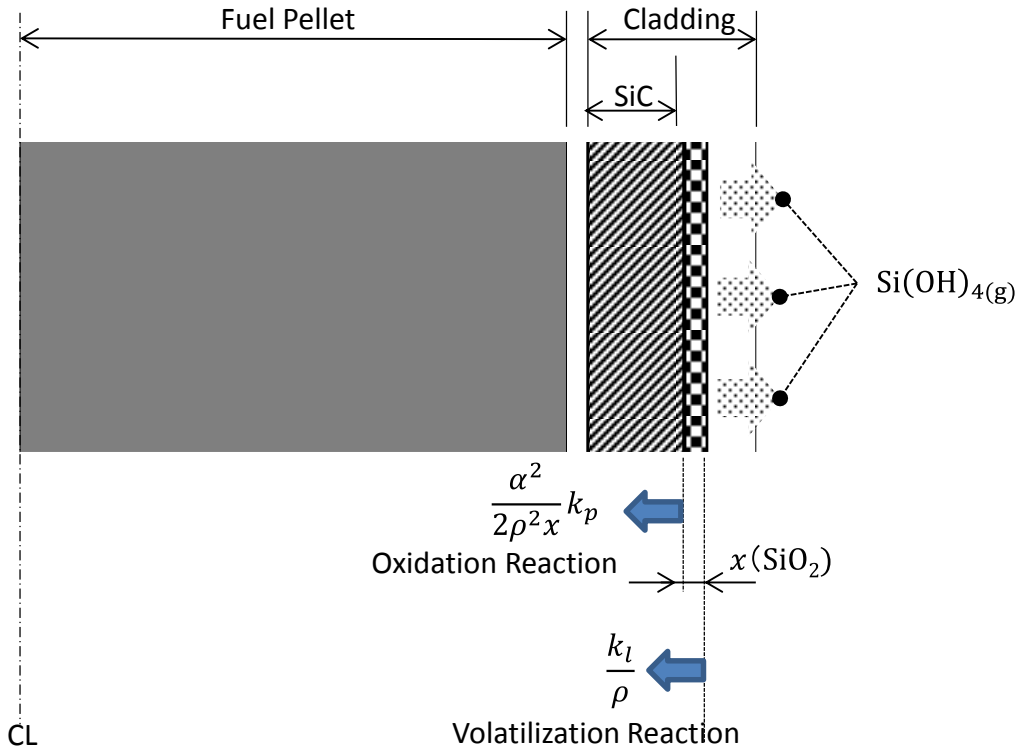

Figure 1 Schematic diagram of SiC oxidation and SiO_2 volatilization

x is the thickness of SiO_2 layer. α is determined from

$$\alpha = \frac{MW_{SiO2}}{MW_{O2} - MW_C} \approx 3, \quad (1)$$

where MW is the molecular weight of the molecule. ρ is the density of SiO_2. k_p is the parabolic oxidation rate constant. k_l is the linear volatilization rate from the surface. The rate of thickness of the SiO_2 oxidation layer is represented as

$$\frac{dx}{dt} = \frac{\alpha^2}{2\rho^2 x} k_p - \frac{k_l}{\rho}. \quad (2)$$

k_p and k_l is represented respectively as

$$k_p = \frac{10^{-4}}{3600} P exp\left(14.13 \pm 3.7 + \frac{-238000 \pm 53000}{RT}\right) \ [kg^2/\ (m^4 s)] \quad (3)$$

and

$$k_l = \frac{10^{-2}}{3600} P^{1.5} v^{0.5} exp\left(19.6 \pm 3.2 + \frac{-211000 \pm 40000}{RT}\right) \ [kg/(m^2 s)], \quad (4)$$

where $R = 8.314\ (J/K/mol)$ is gas constant, $T\ (K)$ is temperature, $P\ (MPa)$ is steam pressure, and $v\ (m/s)$ is gas flow rate.

Because the thickness of the oxidation layer x is very small at the beginning, the oxidation reaction of SiC is dominant at that point. However, as x becomes greater, $\frac{\alpha^2}{2\rho^2 x} k_p$ balances to $\frac{k_l}{\rho}$ because the oxidation reaction term of equation (2) becomes small. The equilibrium thickness of SiO_2 is assumed to x_e. At this time, the thickness of SiC, x_{SiC}, obeys the following differential equation,

$$\frac{dx_{SiC}}{dt} = -\frac{\alpha^2}{2\rho^2 x_e} k_p \approx -\frac{k_l}{\rho}. \quad (5)$$

In the MELCOR model, the oxidation reaction rate is represented as the following equation,

$$\frac{dW^2}{dt} = c_1 exp\left(-\frac{c_2}{T}\right), \quad (6)$$

where W is mass of the oxidized metal per unit area, i.e., W = ρx, and c_1 and c_2 are user-defined variables of the MELCOR.

The left hand side of equation (6) is expanded and is assigned the SiC oxidation reaction rate, which leads to the following equations,

$$\frac{dW^2}{dt} = 2x\rho^2\frac{dx}{dt} = 2x\rho^2\left(-\frac{dx_{SiC}}{dt}\right) = 2x\rho^2\left(\frac{k_l}{\rho}\right) = 2x\rho k_l \approx 2x_e\rho k_l. \quad (7)$$

Here it is assumed that SiO_2 formation rate is equal to SiC oxidation rate in the second equality and that the thickness of SiO_2 is constant in the fifth equality.

The thickness of SiO_2 x_e is assigned $0.28\mu m$ which is determined by experimental conditions. The density of SiO_2, ρ, is assigned $2580\ kg/m^3$ [4]. Because the linear volatilization rate k_l has uncertainties, it is necessary to determine the approximate model. The approximate model for k_l is written below,

$$k_l = \frac{10^{-2}}{3600}P^{1.5}v^{0.5}exp\left(19.6 \pm 3.2 + \frac{-211000 \pm 40000}{RT}\right) \approx \frac{10^{-2}}{3600}P^{1.5}v^{0.5}exp\left(19 + \frac{-211000}{RT}\right) =$$
$$496P^{1.5}v^{0.5}exp\left(\frac{-211000}{RT}\right) = 496P^{1.5}v^{0.5}exp\left(\frac{-25379}{T}\right)[kg/(m^2 s)]. \quad (8)$$

Here, the gas constant $R = 8.314\ (J/K/mol)$ is used for the above equations. dW^2/dt is then written by the following equation,

$$\frac{dW^2}{dt} = 2 \times 0.28 \times 10^{-6} \times 2580 \times 496P^{1.5}v^{0.5}exp\left(\frac{-25379}{T}\right) =$$
$$0.716P^{1.5}v^{0.5}exp\left(\frac{-25379}{T}\right) \quad where \quad c_1 = 0.716P^{1.5}v^{0.5} \quad c_2 = 25379 \quad (9)$$

c_1 and c_2 are input into the MELCOR. The pressure P and the gas flow v are assigned the average value of the time period at which the core heats up. Figure 2 and Figure 3 indicate the maximum core temperature for large break LOCA + ECCS failure + containment spray failure and for Station Blackout (SBO) + auxiliary feedwater failure, respectively. In these figures, current fuel cladding, SiC fuel cladding without considering oxidation reaction, and SiC fuel cladding with considering oxidation reaction are shown. SiC fuel cladding has plenty of time to core melt in comparison to the current fuel cladding. By considering the SiC oxidation reaction, however, time to core melt becomes slightly shorter.

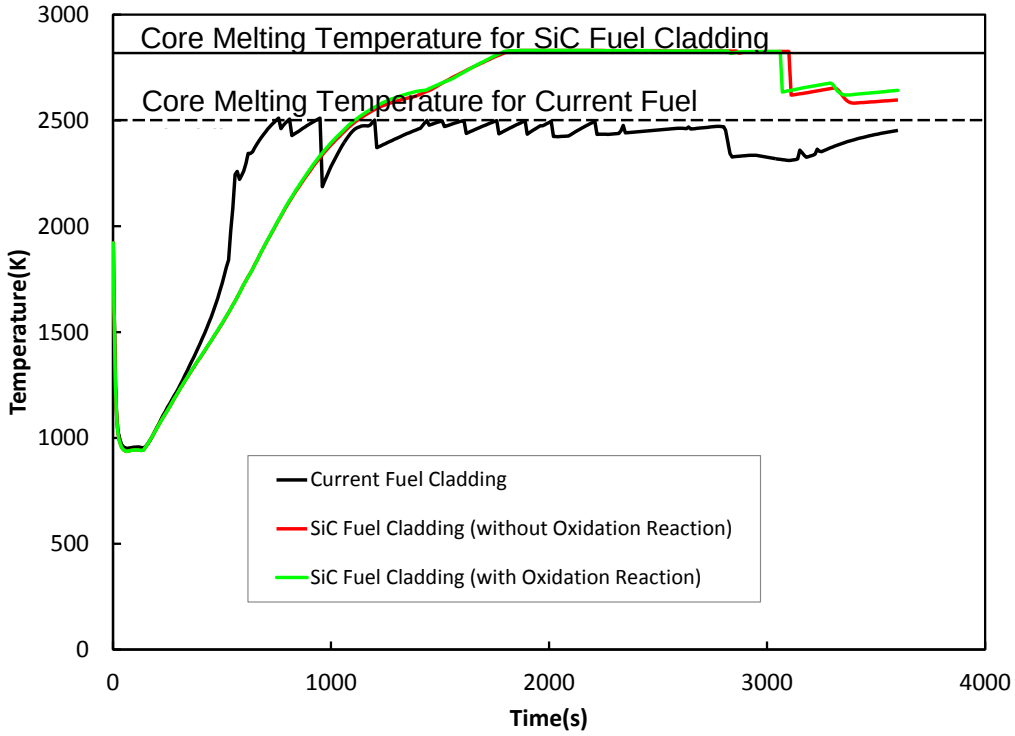

Figure 2 Maximum core temperature of large break LOCA + ECCS failure + containment spray failure for current fuel cladding and SiC fuel cladding

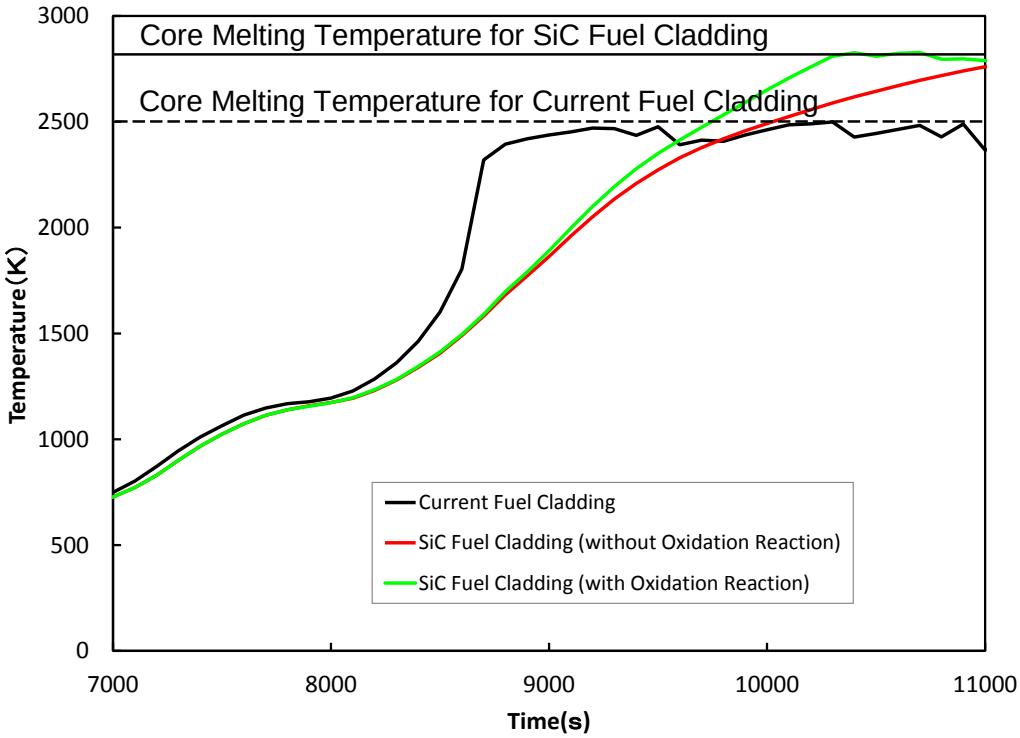

Figure 3 Maximum core temperature of SBO + auxiliary feedwater failure for current fuel cladding and SiC fuel cladding

3. Selected Accident Sequences

There are 15 plant damage states (PDSs) in the PWR plants. PDS is expressed by the characters represented in Table 2. Containment bypass consists of one character. Other PDSs consist of 3 characters.

Table 2 Symbols representing PDS

Items	Characters
Primary system pressure at reactor vessel failure	High : T** Medium : S** Low : A**
Timing of core melt	Early : *E* Late : *L*
Timing of containment failure	Before core melt : **C After core melt : **D, **W, **I
Measures for molten core cooling	Available : **W, **I Not available : **D
Measures for containment cooling	Available : **I Not available : **D, **W
Containment bypass	Interfacing system LOCA : V Steam generator tube rupture : G

*: Arbitrary characters

15 PDSs and their representative accident sequences are shown in Table 3. Of course, each PDS has other accident sequences. For example, A** include medium break LOCA and SED has sequences which include SBO that leads to reactor coolant pump (RCP) seal LOCA.

Table 3 PDSs and their representative accident sequences

PDS	Representative accident sequence
AED	Large break LOCA + ECCS failure + Containment spray failure
AEW	Large break LOCA + ECCS recirculation failure + Containment spray recirculation failure
AEI	Large break LOCA + ECCS failure
ALC	Large break LOCA + High head injection success + Low head injection failure + Containment spray failure
SED	Small break LOCA + ECCS failure + Containment spray failure
SEW	Small break LOCA + ECCS failure + Containment spray recirculation failure
SEI	Small break LOCA + ECCS failure
SLW	Small break LOCA + ECCS recirculation failure + Containment spray recirculation failure
SLI	Small break LOCA + ECCS recirculation failure
SLC	Large break LOCA + High head injection success + Containment spray failure
TED	Transient + Auxiliary feedwater failure + Feed and bleed failure + Containment spray failure
TEW	Transient + Auxiliary feedwater failure + Feed and bleed failure + Containment spray recirculation failure
TEI	Transient + Auxiliary feedwater failure + Feed and bleed failure
V	Interfacing system LOCA + Isolation valve close failure + Cooldown and recirculation failure
G	Steam generator tube rupture + Secondary side open + Cooldown and recirculation failure

There is an idea of selecting AED (large break LOCA) and TED (SBO without RCP seal LOCA) as reference cases in the SA evaluations relating to ATF studies because these are SA sequences in terms of time to core damage and pressure difference between the inside and outside of the fuel cladding. In this study, however, more realistic sequences are selected in terms of frequency of PDS.

In these PDSs shown in Table 3, SED has dominant CDF. Hence accident sequences for ATF studies are selected from SED. The selected accident sequences are as below.

Case A) Small break LOCA + ECCS failure + Containment spray failure
Case B) Small break LOCA + ECCS failure + Containment spray failure + Secondary side cooling success

Here, small break LOCA assumes 2inch hot leg break. In both cases, it is assumed that auxiliary feed water starts up immediately after the accident occurs and that it stops at 5 hours. In the accident sequences with secondary side cooling, steam generator relief valves are opened at 15 minutes after the beginning of the accident.

An accident sequence with high head injection recovery is also considered. This sequence is variation of case B.

Case C) Small break LOCA + ECCS failure + Containment spray failure + Secondary side cooling success + High head injection 1 train recovery

4. Results of Severe Accident analyses for Current Fuel Cladding and for SiC Fuel Cladding

SA analyses are performed for current fuel cladding and for SiC fuel cladding by using MELCOR. As stated previously, material properties and oxidation reaction rate of cladding are modified from current fuel cladding without changing the MELCOR source code. The pressure and the gas flow rate are determined from the average value of the time period during which the core heats up. Table 4 shows the event summary of each case. Figure 4 and Figure 5 show the maximum core temperature and the hydrogen generation mass, respectively.

For the SiC fuel cladding, the maximum core temperature rises slowly because of the relatively small oxidation reaction rate. The time to core melt is delayed from 5.0 hours to 7.6 hours for case A and from 13.0 hours to 14.6 hours for case B. For current fuel cladding, it is assumed that core melt occurs when the maximum core temperature reaches the temperature at which the cladding is not able to stand upright. For SiC fuel cladding, it is assumed that core melt occurs when the maximum core temperature reaches the SiC melting temperature. While time to core melt is delayed tens of minutes for large break LOCA and SBO, time to core melt is delayed 2.6 hours for case A (small break LOCA) and 1.6 hours for case B (small break LOCA with secondary cooling). This is because, in case A, the core is cooled by intermittent accumulator injection for a relatively long time. For case B, accumulator injection is completed at the beginning because the primary side pressure is decreased by secondary side cooling. The secondary side cooling can cool the core for a relatively long time. For these reasons, the effect of the difference in oxidation reaction rate between current fuel cladding and SiC fuel cladding appears significantly in the small LOCA sequences. In the accident sequences selected from SED which is a dominant PDS, the advantage of SiC fuel cladding is clarified.

Because time to core melt is delayed several hours in case A and case B, accident management can be taken into account during the delay time. Case C is an accident sequence based on case B which assumes that the high head injection recovers at the time when core melt occurs for current fuel cladding. The maximum temperature for SiC fuel cladding of case C decreases rapidly after high head injection recovers without leading to core melt. The achieving temperature is sufficiently low compared with the core melting temperature of SiC fuel cladding.

Oxidation reaction rate for SiC fuel cladding is smaller than for current fuel cladding. That is why hydrogen generation in the core is small for SiC fuel cladding. In each sequence, hydrogen generation mass is reduced significantly. There is still hydrogen generation for the SiC fuel cladding because considerable core structures are oxidized by hot steam. Especially in case C in which high head injection recovers, hydrogen generation mass for SiC fuel cladding is reduced to about one-sixth of that for current fuel cladding. As seen from the above, by employing SiC fuel cladding, hydrogen concentration in the containment becomes low and the possibility of hydrogen burn or containment failure by hydrogen explosion is eliminated. These results suggest that countermeasures against hydrogen explosion such as igniter and passive recombiner can be reduced by decreasing of hydrogen generation.

As stated above, employing SiC fuel cladding as ATF has advantages in terms of expansion of time to core melt and reduction of hydrogen generation especially in the realistic accident sequences of high CDF.

Table 4-a Event summary (case A)

Events	Time	
	Current fuel cladding	SiC fuel cladding
Accident occurs	0 sec	0 sec
Reactor trip	1.0 s	1.0 s
SI signal	1.9 min	1.9 min
Core melt	5.0 hr	7.6 hr
Lower core support plate failure	8.8 hr	9.0 hr
Reactor vessel failure	8.8 hr	9.0 hr

Table 4-b Event summary (case B)

Events	Time	
	Current fuel cladding	SiC fuel cladding
Accident occurs	0 sec	0 sec
Reactor trip	1.0 s	1.0 s
SI signal	1.9 min	1.9 min
Core melt	13.0 hr	14.6 hr
Lower core support plate failure	16.2 hr	18.0 hr
Reactor vessel failure	16.3 hr	18.1 hr

Table 4-c Event summary (case C)

Events	Time	
	Current fuel cladding	SiC fuel cladding
Accident occurs	0 sec	0 sec
Reactor trip	1.0 s	1.0 s
SI signal	1.9 min	1.9 min
Core melt	13.0 hr	N/A
Lower core support plate failure	N/A	N/A
Reactor vessel failure	N/A	N/A

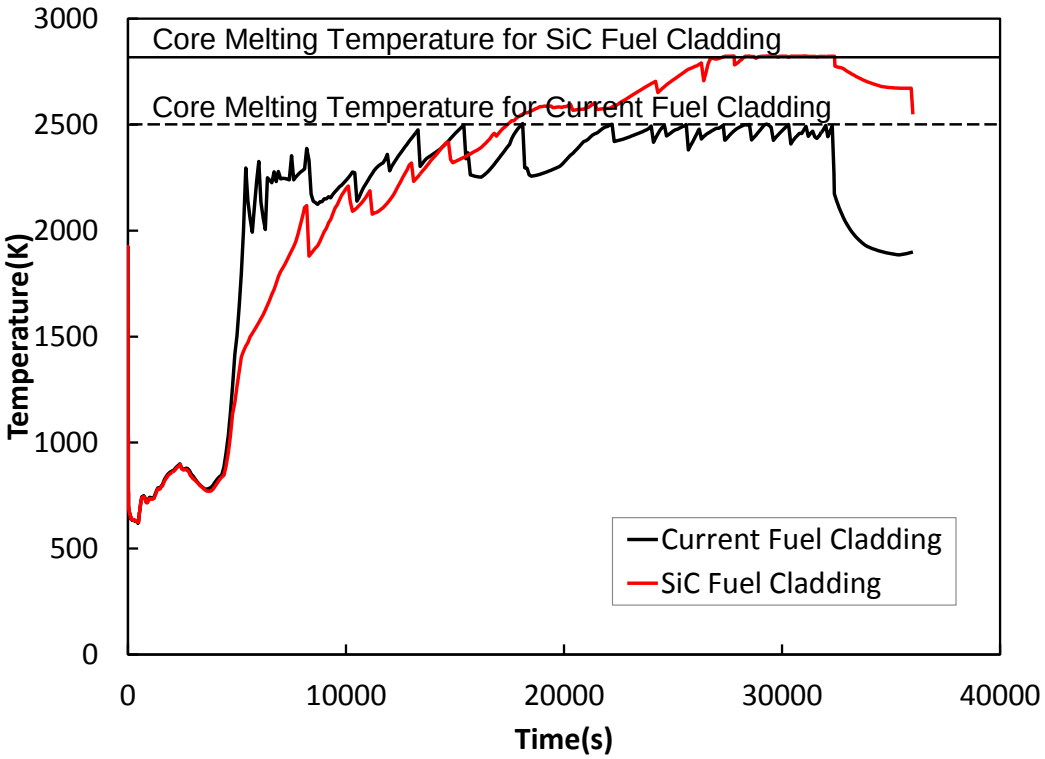

Figure 4-a Maximum core temperature for current fuel cladding and SiC fuel cladding (case A)

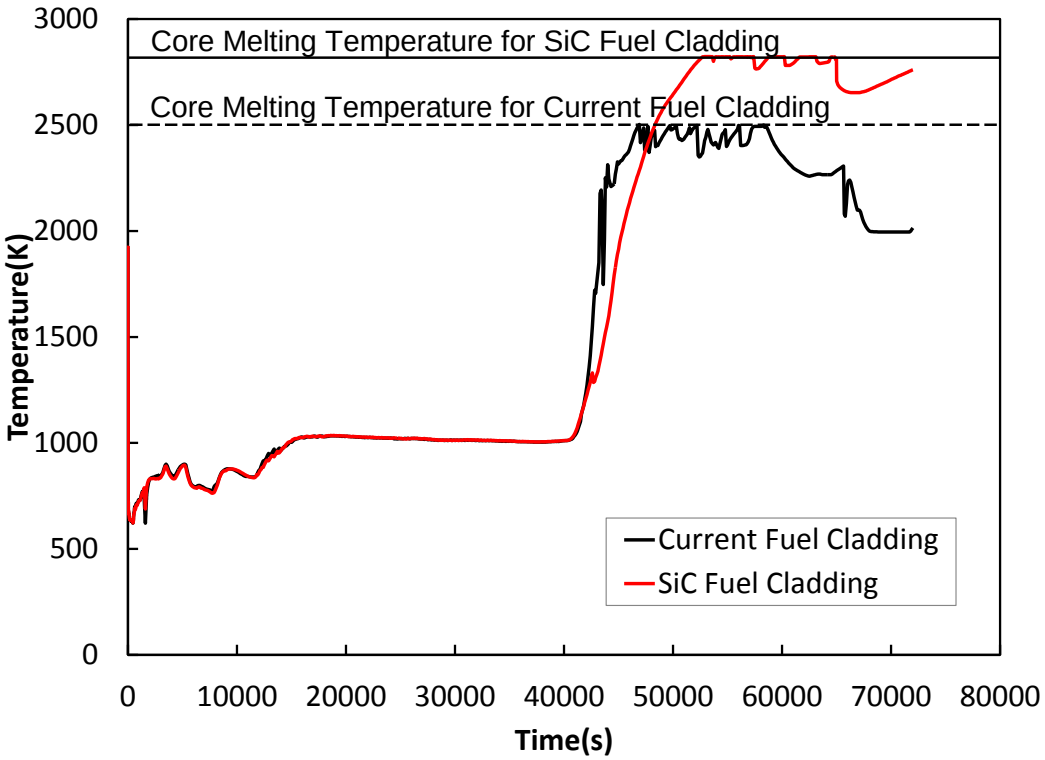

Figure 4-b Maximum core temperature for current fuel cladding and SiC fuel cladding (case B)

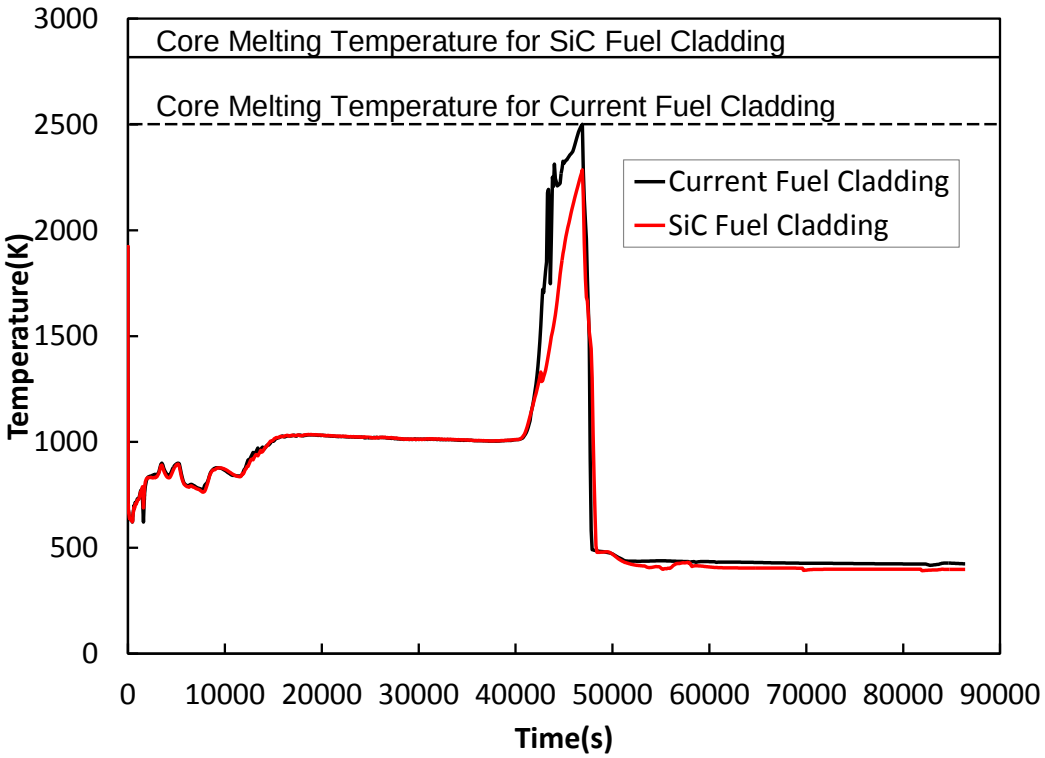

Figure 4-c Maximum core temperature for current fuel cladding and SiC fuel cladding (case C)

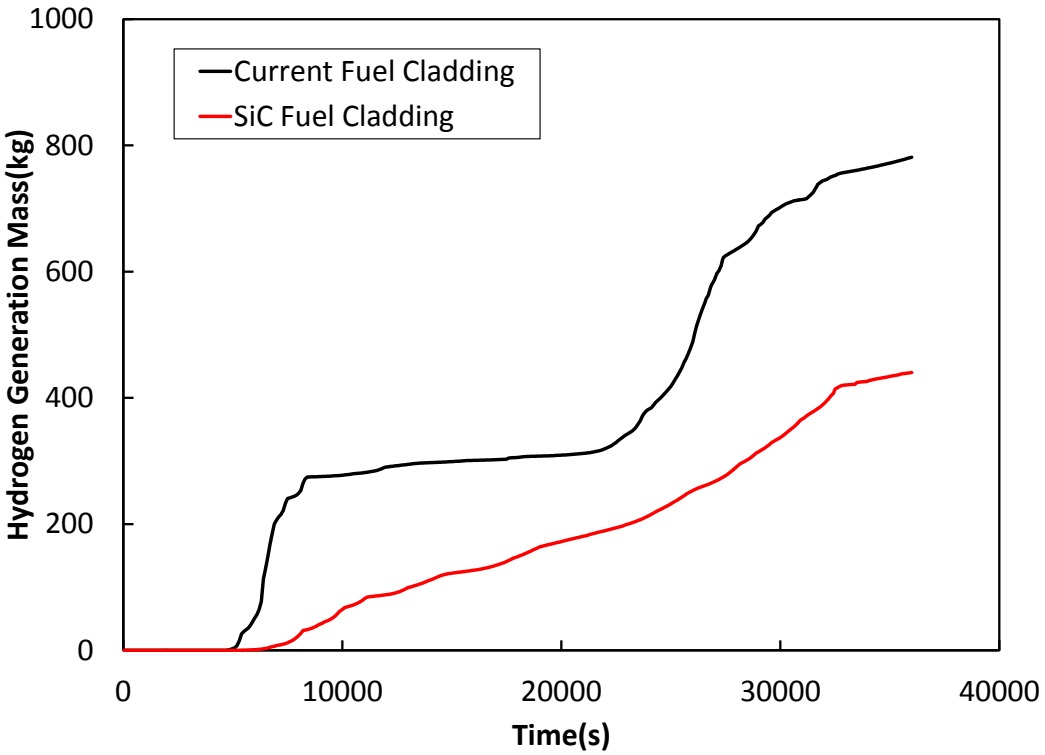

Figure 5-a Hydrogen generation mass for current fuel cladding and SiC fuel cladding (case A)

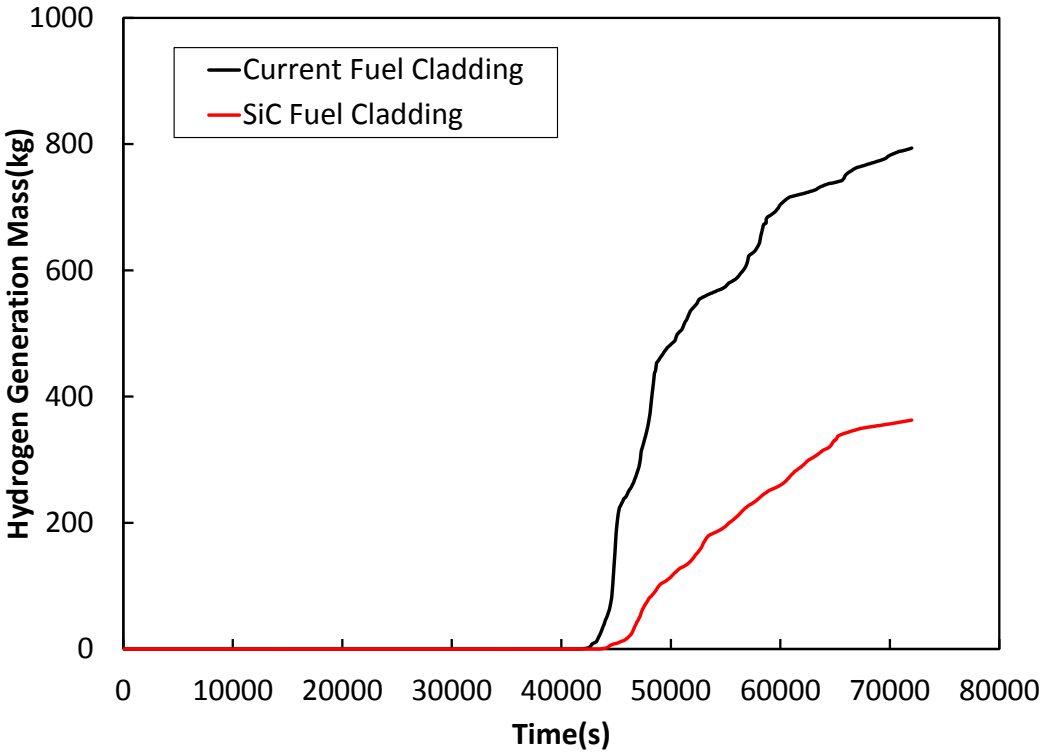

Figure 5-b Hydrogen generation mass for current fuel cladding and SiC fuel cladding (case B)

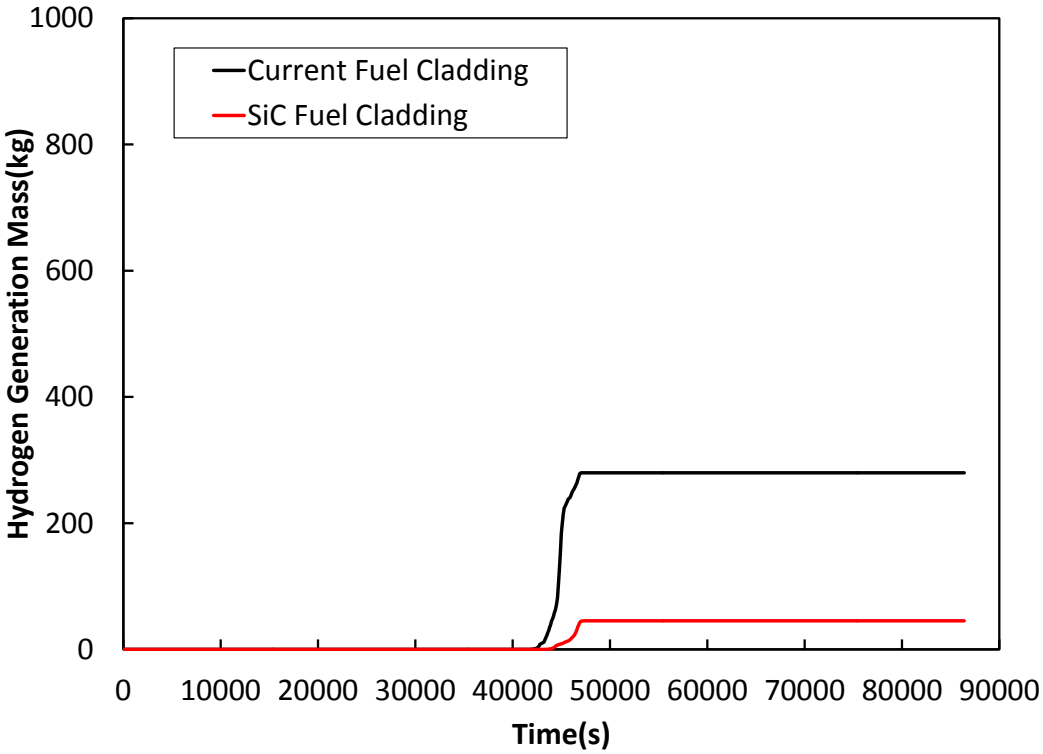

Figure 5-c Hydrogen generation mass for current fuel cladding and SiC fuel cladding (case C)

5. Summary

Material properties and oxidation reaction rate of current fuel cladding were changed in order to model SiC fuel cladding in the input of MELCOR. By using the MELCOR in which the input is modified, the advantage of SiC fuel cladding was clarified for dominant PDS in terms of time to core melt and hydrogen generation.

The oxidation reaction rate of SiC is proportional to 1.5^{th} of the steam pressure. Therefore, when the steam pressure is high enough, the oxidation reaction rate becomes high and hydrogen generation increases. It is expected that experimental knowledge about dependence of the steam pressure is improved.

6. References

[1] L. L. Snead et al., “Handbook of SiC properties for fuel performance modeling”, J. Nucl. Mater. 371, 329-377 (2007)

[2] Yutai Katoh et al., “Continuous SiC fiber, CVI SiC matrix composites for nuclear applications : Properties and irradiation effects”, J. Nucl. Mater. 448, 448-476 (2014)

[3] K. A. Terrani et al., “Silicon carbide oxidation in steam up to 2MPa”, J. Am. Ceram. Soc. 97 (8) 2331-2352 (2014)

[4] JSME Data Book, “Heat Transfer”, 4^{th} Edition (1986)